EQUIPMENT FOR FLOW DIAGNOSTICS AND CONTROL

by

Professor Mo Samimy
Gas Dynamics and Turbulence Laboratory
Department of Mechanical Engineering
The Ohio State University
2300 West Case Road
AARL/GDTL
Columbus, Ohio 43235
Tel: 614-292-6988; Fax: 614-292-5552
E-mail: Samimy.1@osu.edu

REPORT DOCUMENTATION PAGE

AFRL-SR-AR-TR-06-0011

Public reporting burden for this collection of information is estimated to average 1 hour per response, including the time for reviewing instructions, searching exist
the collection of information. Send comments regarding this burden estimate or any other aspect of this collection of information, including suggestions for
Operations and Reports, 1215 Jefferson Davis Highway, Suite 1204, Arlington, VA 22202-4302, and to the Office of Management and Budget, Paperwork Redu

1. AGENCY USE ONLY *(Leave blank)*	2. REPORT DATE	3. REPORT TYPE
		Final

4. TITLE AND SUBTITLE	5. FUNDING NUMBERS
Equipment for Flow Diagnostics and Control	FA9550-04-1-0275

6. AUTHOR(S)

Dr. Samimy

7. PERFORMING ORGANIZATION NAME(S) AND ADDRESS(ES)	8. PERFORMING ORGANIZATION REPORT NUMBER
Ohio State University	

9. SPONSORING/MONITORING AGENCY NAME(S) AND ADDRESS(ES)	10. SPONSORING/MONITORING AGENCY REPORT NUMBER
AFOSR-Lt. Col Sharon Heise	

11. SUPPLEMENTARY NOTES

12a. DISTRIBUTION AVAILABILITY STATEMENT	12b. DISTRIBUTION CODE
Approved for public release, distribution unlimited	

13. ABSTRACT *(Maximum 200 words)*

The DURIP grant enabled us to acquire a complete and powerful stereo Particle Imaging Velocity (PIV) system, equipment for experimentally implementing real-time feedback flow control, and all the necessary equipment for automatic control of the flow facilities at the Gas Dynamics and Turbulence Laboratory (GDTL). All of these equipment items enabled us to get detailed Ply measurements simultaneously with pressure measurements. We then used the techniques described in the rest of this report to obtain the first experimental results based reduced order model and controller based on the model. We have successfully implemented the controller with very encouraging results. The results presented in this report of based two papers: one we presented in an AIAA conference last summer (Caraballo et al. 2005) and one we will present in another AIAA conference in early January 2006 (Caraballo et al. 2006).

14. SUBJECT TERMS		15. NUMBER OF PAGES
		16. PRICE CODE

17. SECURITY CLASSIFICATION OF REPORT	18. SECURITY CLASSIFICATION OF THIS PAGE	19. SECURITY CLASSIFICATION OF ABSTRACT	20. LIMITATION OF ABSTRACT

Standard Form 298 (Rev. 2-89) (EG)
Prescribed by ANSI Std. 239.18
Designed using Perform Pro, WHS/DIOR, Oct 94

ABSTRACT

The DURIP grant enabled us to acquire a complete and powerful stereo Particle Imaging Velocity (PIV) system, equipment for experimentally implementing real-time feedback flow control, and all the necessary equipment for automatic control of the flow facilities at the Gas Dynamics and Turbulence Laboratory (GDTL). All of these equipment items enabled us to get detailed PIV measurements simultaneously with pressure measurements. We then used the techniques described in the rest of this report to obtain the **first experimental results based reduced order model and controller based on the model**. We have successfully implemented the controller with very encouraging results. The results presented in this report of based two papers: one we presented in an AIAA conference last summer (Caraballo et al. 2005) and one we will present in another AIAA conference in early January 2006 (Caraballo et al. 2006).

In this report results for subsonic cavity flow control using a reduced-order model based feedback control derived from experimental measurements. The model was developed using the Proper Orthogonal Decomposition of PIV images in conjunction with the Galerkin projection of the Navier-Stokes equations onto the resulting spatial eigenfunctions. A linear-quadratic optimal controller was designed to control the time coefficient and tested in the experiments. The stochastic estimation method was used for real-time estimation of the corresponding time coefficients from 4 dynamic surface pressure measurements. The results obtained showed that controller was capable of reducing the cavity flow resonance at the design Mach 0.3 flow, as well as at other flows with slightly different Mach number. In the present work we present several improvement made to the method. The reduced order model was derived from a larger set of PIV measurements and we used 6 sensors for the stochastic estimation of the instantaneous time coefficients. The reduced order model so obtained showed a better convergence of the time coefficients. This combined with the 6-sensor estimation improved the control performance while using a scaling factor closer to the theoretically expected value. The controller also performed better for the off design flow conditions.

ACKNOWLEDGMENTS

I. INTRODUCTION

In this report, we present and discuss recent progress obtained applying state estimation and proper orthogonal decomposition (POD) in the development and experimental validation of a reduced-order model based control of subsonic flow over a shallow cavity. This work continues and expands our previous ones based on numerical data (Yuan et al. 2005) and experimental data (Caraballo et al. 2005) towards the design and implementation of a feedback controller by applying system identification and modeling techniques to direct measurements of physical flow quantities. This work is part of a larger multidisciplinary effort in the development of a basic understanding and implementation of feedback flow control techniques (Samimy et al. 2004).

Successful application of feedback control is widespread in areas such as robotics, aerospace, telecommunication, transportation systems, manufacturing systems, and chemical processes. Recently, various attempts have been made to apply feedback control techniques to aerodynamic flow phenomena (Gad-El-Hak 2000, Cattafesta et al. 2003). In contrast with open-loop flow control, which can produce useful results but lacks the responsiveness or the flexibility needed for application in dynamic flight environments, closed-loop flow control appears to be suited for the successful management of flow in many applications due to its adaptability to variable conditions and to its potential for significantly reducing the power required for controlling the flow (Cattafesta et al. 1997). However, the tools of classical control systems theory are not directly applicable to fluid flow systems which display spatial continuity and nonlinear behavior, and pose formidable modeling challenges due to their infinite dimensionality, the complexity introduced by the Navier-Stokes equations, and the peculiar characteristics of the measurement and actuation devices. In order to design and successfully implement a closed-loop control strategy, it is necessary to obtain simple dynamical models of the system, which on one hand capture the important dynamic characteristics of the flow and the effect of the actuation, and on the other hand are simple enough to be used for model-based feedback control.

The benchmark case selected in our study is the flow over a shallow cavity (Samimy et al. 2004), a configuration present in many practical applications that benefits from having been extensively studied by several researchers (e.g. Rossiter 1964, Heller and Bliss 1975, Cattafesta et. al. 2003). This flow is characterized by a strong coupling between flow dynamics and flow generated acoustic field that produces a self-sustained resonance known to cause, among other problems, store damage and airframe structural fatigue in weapons bays. A comprehensive review of this phenomenon and of different control and actuation strategies developed for its suppression is given in Cattafesta et al. (2003).

The approach we follow in the development of a reduced order model for the cavity flow is based on proper orthogonal decomposition (POD). This technique extracts information on the coherent structures, which are the most dominant characteristic of the flow and the only entities that can effectively be controlled, on the basis of the spatial correlation tensor of the velocity field in the flow. It represents the dynamics of flow field as a set of spatial eigenmodes that are modulated by time coefficients obtained by projecting the instantaneous flow fields onto the POD basis. Obtaining a time varying description would require simultaneous, real-time flow measurements at every spatial point. While this is feasible using data from numerical simulations, it becomes an extremely challenging task with data obtained experimentally even in low-speed flows (Thurow et al. 2005). In this case the obstacle can be surmounted by exploiting stochastic estimation methods that correlate the velocity field with a variable that can be measured continuously in time, such as surface pressure (Glauser et al. 2004, Ukeiley and Murray 2005, Caraballo et al. 2005, and).

The state equation employed for controller design is in the form of a system of nonlinear ordinary differential equations for the time coefficients. It is obtained by projecting the governing flow equations with velocities approximated by the POD description onto the spatial basis using the Galerkin projection

method. The system of equations can be recast in a form expressing the control input explicitly as required to apply the tools of control theory for the development of feedback control.

The procedure that we are using is summarized here (Caraballo et al. 2005). The state equation (i.e. the POD time coefficients) was estimated in real-time by employing the stochastic estimation technique with correlations obtained from off-line simultaneous particle image velocimetry (PIV) and dynamic pressure measurements at several locations on the surface of the cavity.

Equilibrium analysis led to the linearization of the reduced-order model around the equilibrium point. A simpler model for controller design was then obtained by shifting the origin of the coordinates to the equilibrium point. This corresponds to removing the effect of the mean flow from the low-order model, and considering the local behavior of the system around the mean flow. The availability of real-time estimates of the state of the model allowed the use of linear state feedback control. To this aim we designed and tested experimentally a linear-quadratic optimal state feedback controller.

From the results obtained we can conclude that the controller significantly reduces the resonance peak of the Mach 0.3 single Rossiter mode, for which it was designed, by switching it to a multi-mode resonance. The controller seems to be quite robust, as it can control the flow with some variations in the flow Mach number. This is an ongoing research effort. In this report we present further improvement to the technique that we have developed and used.

In the next sections we will introduce the flow facility used in this study and then focus on the POD and Galerkin methods adopted for deriving the reduced-order model and the stochastic estimation approach used for real-time estimate of the model variables directly from dynamic pressure measurements. This is followed by the design and application of the linear-quadratic controller and by the presentation and discussion of the results.

II. EXPERIMENTAL FACILITY

The experimental facility is described in detail in Debiasi and Samimy (2004). It is an instrumented, optically accessible wind-tunnel that operates in a blow-down fashion with atmospheric exhaust. The filtered, dried air is conditioned in a stagnation chamber before entering a smoothly contoured converging nozzle to the 2 inch by 2 inch test section. The facility can run continuously in the subsonic range between Mach 0.25 and 0.70 and transonic and supersonic applications are possible by changing modular components.

A shallow cavity is recessed in the test section with a depth D = 12.7 mm and length L = 50.8 mm for a length to depth aspect ratio L/D = 4. For control the cavity shear-layer receptivity region is forced by a 2-D synthetic-jet type actuator issuing at 30 degrees relative to the main flow from a 1 mm slot embedded in the cavity leading edge and spanning the width of the cavity, Fig. 1. A Selenium D3300Ti compression driver provides the mechanical oscillations necessary to create the zero net mass, non-zero net momentum flow for actuation. The actuator signals are produced by either a BK Precision 3011A function generator for open-loop forcing or by a dSPACE 1103 DSP control board in closed-loop studies and are amplified by a Crown D-150A amplifier. All these have been acquired using DURIP funding.

The "snapshots" of the flow field, required for the development of the low dimensional model, are acquired and processed using a LaVision Inc. PIV system. Again, the PIV system was acquired using DURIP funding. Details of the PIV system, procedure, and results are presented in Little et al. (2006). The main flow is seeded with Di-Ethyl-Hexyl-Sebacat (DEHS) particles by using a 4-jet atomizer upstream of the stagnation chamber. This location allows homogenous dispersion of the submicron particles throughout the test section. A dual-head Spectra Physics PIV-400 Nd:YAG laser operating at the 2nd harmonic (532 nm) is used in conjunction with spherical and cylindrical lenses to form a thin (~1mm), vertical sheet spanning the streamwise direction of the cavity at the middle of test section width. In order to minimize beam reflections, a small slot cut into the cavity floor allows the laser sheet to exhaust and diffuse in a sealed light-trap. The time separation between the lasers pulses used for PIV can be tuned according to the flow velocity. For Mach 0.30 flow this value is 1.8 microseconds. Two images corresponding to the pulses from each laser head were acquired by a 2000 by 2000 pixel CCD camera equipped with a 90 mm macro lens with a narrow band-pass optical filter. The images were divided into 32 by 32 pixel interrogation windows which contained 6-10 seed particles each. For each image sub regions were cross correlated by using multi-pass processing with 50% overlap. The resulting vector fields were post-processed to remove any remaining spurious vectors. This setup gave a velocity vector grid of 128 by 128 over the measurement domain of 50.8 mm which translates to each velocity vector being separated by approximately 0.4 mm.

Flush-mounted Kulite transducers were placed on various locations on the walls of the test section for dynamic pressure measurements. Figure 2 shows the locations of the transducers used in this study. All these transducers have an almost flat frequency response up to about 50 kHz and are powered by a dedicated signal conditioner that amplifies and low-pass filters at 10 kHz their signals.

For state estimation, dynamic pressure measurements were recorded simultaneously with the PIV measurements using a National Instruments (NI) PCI-6143 S-Series data acquisition board mounted on a Dell Precision Workstation 650. The system allows synchronous sampling of 8 channels with a maximum sampling frequency of 250 kHz per channel. Each pressure recording was band-pass filtered between 100 Hz and 10 kHz to remove spurious frequency components. In the current study 1000 PIV snapshots were recorded for each flow/actuation condition explored. For each PIV snapshot 128 pressure samples from the laser Q-switch signal and from each of the transducers of Fig. 2 were acquired at 50 kHz. The NI board was triggered by a programmable timing unit (PTU) housed in the PIV system that activated the beginning of the acquisition to allow the Q-switch TTL to fall approximately in the middle of the 256

data points. The simultaneous sampling of the laser Q-switch signal with the pressure signals allows for each snapshot the identification of the section of pressure time-traces corresponding to the instantaneous PIV velocity field. Additional, longer recordings of 262,144 samples per channel acquired at 200 kHz were also used to derive SPL spectra as described in Debiasi et al. (2004).

For closed-loop control of the flow a dSPACE 1103 DSP board connected to the Dell Precision Workstation 650 was used (all acquired via DURIP funding). This system utilizes four independent, 16-bit A/D converters each with 4 multiplexed input channels and allows simultaneous acquisition and control processing of 4 signals and almost simultaneous, due to multiplexing, acquisition and processing of additional signals at a rate up to 50 kHz per channel to produce at the same rate a control signal from a 14-bit output channel. Similar to state estimation pressure data, the pressure signals were band-pass filtered between 100 Hz and 10 kHz to remove spurious frequency components.

III. REDUCED-ORDER MODELING

Reduced-order models of the flow were derived from PIV and surface pressure measurements of the cavity flow as described by the authors in previous works (Samimy et al. 2004, and Caraballo et al. 2004, 2005). The approach is based on the combination of three separate tools. First, the POD method is used to obtain a spatial basis of the flow. Then, the POD expansion is combined with the Galerkin projection method to obtain the flow model which consists of a set of ordinary differential equations for the POD temporal coefficients. In this set of equations the control input appears explicitly to facilitate the design of the feedback control algorithm. Finally stochastic estimation is used to estimate these temporal coefficients based on real time surface pressure measurements.

POD Method

This is the first tool used to obtain the reduced-order model. In recent years POD has been used in the study of several turbulent flows and in the development of feedback control for them. The method was introduced by Lumley (1967) as an objective way to extract large scale structures in a turbulent flow. The technique originally was developed for data sets of large sample time $\mathcal{T}$ at a few spatial locations $\mathcal{L}$. More details on the fundamentals of this method can be found in Holmes et al. (1996) and Delville et al. (1998). The POD approach used in this investigation is the snapshot method of Sirovich (1987), which is an alternative way of obtaining the POD modes more suitable for highly spatially resolved data sets ($\mathcal{L} >> \mathcal{T}$) that can be obtained using numerical simulations or advanced laser-based flow diagnostics. A detailed description of the application of the Sirovich POD method to the current study case is given in Samimy et al. (2004) and Caraballo et al. (2004).

The POD method aims to describe the temporal-spatial evolution contained in $\mathcal{T}$ realizations of the fluctuating components of a flow variable (e.g. the fluctuating component u' of the streamwise velocity u) as combination of $N < \mathcal{T}$ spatial modes (or eigenfunctions) $\varphi_i(x)$, i.e. a reduced basis of modes that capture the coherent structures, the dominant features, present in the flow:

$$u'(x,t) \cong \sum_{i=1}^{N} a_i(t)\varphi_i(x) \qquad (3.1)$$

The time coefficients $a_i(t)$ are functions of time only and capture the time evolution of the corresponding coherent structures. The number of modes, N, used depends on the nature of the problem and the purpose of the model. The time coefficients of a known instantaneous flow filed can be obtained from;:

$$a_i(t) = \int_D u'(x,t)\varphi_i^*(x)dx \qquad (3.2)$$

where * denotes complex conjugate. Equation (3.2) requires that the instantaneous flow field be measured or numerically calculated simultaneously at every point in the flow domain of interest.

For each of the flow conditions explored in this work, 1000 PIV snapshots of the flow field were acquired as described in the previous section and used in the derivation of the modes and their time coefficients. The increased number of snapshot compared to that (500) used in Caraballo et al. (2005) allowed complete convergence of the average turbulent kinetic energy of the flow in the shear layer region. Figure 3 shows how the mean turbulent kinetic energy at different location on the shear layer converges when more than 700 images are used. Figure 4 shows the first two modes of the normal velocity of the cavity flow using 500 and 1000 snapshots. It can be noticed how increasing the number of snapshots helps to smooth out the structures capture by the modes, as the small scale effects are captured

by the higher modes added to the system. However, as it was noticed before (Caraballo et al 2005), there is a small effect on the energy content of the modes, especially for the lower order modes.

Galerkin Projection and Low Dimensional Model

The Galerkin projection method was used to obtain a reduced-order model of the cavity flow consisting of a system of ordinary differential equations for the time coefficients $a(t)=[a_1(t) \ a_2(t) \ \ldots \ a_N(t)]$. The method relies on the projection of the governing equations of the flow, the compressible Navier-Stokes in this case, onto the basis of POD modes. Detailed explanation on the derivation of this model is given in our earlier work (Samimy et al. 2004, and Caraballo et al. 2004). The form of the equations used here is based on the work of Rowley (2002), where the compressible Navier-Stokes equations are simplified and written as:

$$\frac{Dc}{Dt} + \frac{\gamma-1}{2} c \, \nabla \bullet u = 0$$

$$\frac{Du}{Dt} + \frac{2}{\gamma-1} c \nabla c = \frac{\mu}{\rho} \nabla^2 u \qquad (3.3)$$

where $u = (u, v)$ is the velocity vector and c is the local speed of sound.

To apply the Galerkin method, first each flow variable is decomposed into its mean and fluctuating components, and then the POD expansion equation (3.1) is written for each of the fluctuating components. Next, the flow variables in (3.3) are replaced by the expanded expressions of mean and fluctuating components. The new form of the governing equations is then projected onto the basis of POD modes by taking the inner product of each term with the POD modes according to the vector norm (Rowley, 2002). This procedure yields a system of equations in which the control input is not separated from the rest of the flow, i.e. the control effect is implicit in the model. This is not useful for control law design. In order to derive a model where the control input appears explicitly in the equations, the sub-domain of space where the control is introduced is separated from the rest of the field (Caraballo et al. 2005) which yields a system in the following form:

$$\dot{a}(t) = F + Ga(t) + \begin{bmatrix} a^T(t)H^1 a(t) \\ \vdots \\ a^T(t)H^N a(t) \end{bmatrix} + B\Gamma(t) + \begin{bmatrix} \left(\overline{B}^1 \Gamma(t)\right)^T a(t) \\ \vdots \\ \left(\overline{B}^N \Gamma(t)\right)^T a(t) \end{bmatrix}, \qquad 3.4)$$

where the matrices of constant coefficients F, G, H^i, B and $\overline{B}^i$, $i=1,\ldots N$, are obtained from the Galerkin projection, and Γ is the control input applied at the forcing location, Yuan et al. (2005). Equation (3.4) represents a model of the cavity flow in terms of the time coefficients $a(t)$ obtained with POD from $\mathcal{T}$ time uncorrelated PIV data sets.

Using a finite number N of modes to describe the flow not only loses some flow details but also the energy transfer process between the N retained modes and the neglected ones. Therefore an additional viscous term, modal eddy viscosity (Noack et al. 2004), was added to the model to maintain the overall flow energy balance and to compensate for other small errors introduced in the derivation of the model. This additional viscous term is added to the viscous term present in the flow equation, and is obtained by a modal energy balance as presented in Noack et al. 2004.

The system (3.4) was solved to check the evolution and convergence of the time coefficients and to compare it to the corresponding values obtained with (3.2) from the PIV snapshots. The time coefficients evolved to bounded values in most cases when 4 thru 10 modes were used in (3.4), the solution did not converge for 7 modes. Figure 5 shows the evolution of the time coefficient of the first mode for the

baseline Mach 0.3 flow when using $N = 4$. After an initial transient this coefficients oscillates around close to zero with an amplitude comparable to the time coefficients obtained with (3.2) from the PIV snapshots. This is a better result than the one we previously obtained by using 500 snapshots of the same flow (Caraballo et al, 2005) which is also shown in Fig. 5. However, we observed that the frequency of oscillation of the new set is slightly lower than the experimental value, which we relate to the additional dissipation introduced into the model. It was observed that the system converged to the same values irrespective of the initial condition of the time coefficient used for the solution of (3.4). Similar results were obtained for the time coefficients of the other three modes of the baseline Mach 0.3 flow, and for the modes of the same flow with different types of forcing.

The overall effect that these improvements had in the controller design and implementation will become clear later. Finally, we elected to use the $N = 4$ for the model used to design the controller so to simplify the control algorithm and its experimental implementation.

Stochastic Estimation

For the implementation of the controller, the real-time knowledge of the time coefficient is required. To achieve this we used Stochastic Estimation (SE). Stochastic estimation, proposed by Adrian (1979) as another method to extract coherent structures from a turbulent flow field, estimates flow variables at any location by using the information, including statistical information, about the flow at a limited number $\mathcal{L}^*$ of locations. The method has been used to study various flows (e.g. Adrian and Moin 1988, Cole and Glauser 1998), and as a complementary tool for POD to estimate its time coefficients from experimental measurements in subsonic jets (Picard and Delville, 2000) and in cavity flows (Ukeiley and Murray, 2005, and Samimy et al 2004). In recent years it has also been used to estimate the time coefficient for feedback control of the flow (Glauser et al. 2004, Siegel et al. 2005, and Caraballo et al. 2005).

We used quadratic SE to estimate the time coefficients of the flow model (3.4) directly from real-time surface pressure measurements at a limited number $\mathcal{L}^*$ of locations. The estimation can be written in the following form:

$$\hat{a}_i(t) = C_{ik}\, p_k(t) + D_{ikl}\, p_k(t) p_l(t) \qquad i=1\ldots N, \qquad k,\, l\ldots = 1\ldots \mathcal{L}^*$$

$$,\qquad (3.5)$$

where $C, D\ldots$ are the matrices of the estimation coefficients obtained by minimizing the average mean square error e_i between the values of $a_i(t_r)$ obtained with (3.2) at the times of PIV capture and the estimated ones $\hat{a}_i(t_r)$ at the same times,

$$e_i = \left\langle \left[\hat{a}_i(t_r) - a_i(t_r) \right]^2 \right\rangle \qquad r = 1\ldots \mathcal{T},$$

$$(3.6)$$

To calculate the matrices of (3.5) only $\mathcal{L}^*$ pressure values taken simultaneously with of PIV measurements were used from each of the 1000 simultaneous PIV-pressure acquisitions. The procedure to obtain the estimation matrices is described in more detail in Caraballo et al. (2004). With our experimental setup, real-time measurements of the surface pressure were obtained at the $\mathcal{L}^* = 6$ locations of interest in the cavity test section shown in Fig. 2.

The stochastic estimation method has been previously tested for the cavity flow under investigation, showing good agreement in the estimation of the time coefficient based on the surface

pressure (Caraballo et al. 2005). When the method was applied to the new data set the estimated coefficients of all four modes remained close the values obtained from the PIV images.

IV. CONTROLLER DESIGN AND IMPLEMENTATION

In this section, we present our model based controller design approach and real time implementation results. The control design approach has been presented in Yuan et al. (2005) and Caraballo et al. (2005) in details, which includes equilibrium computation, coordinates transformation, linear approximation and linear-quadratic state feedback control design. In this work, the same control design procedure was followed on a large experimental data set (PIV data) derived Galerkin model. The real time implementation of the new controller showed improvement of the preliminary results presented in Caraballo et al. (2005). The reference flow model used here for control design is a nonlinear 4-dimensional state space model for the baseline flow at Mach 0.3, which is given by (3.4) with $N = 4$.

Equilibrium analysis and model simplification

Performing and equilibrium analysis and coordinate transformation on model (3.4), the constant term F is removed, *i.e.*, moving the coordinate origin to the equilibrium point, therefore simplifying the state space model. The simplified model in the new set of coordinates $\tilde{a} = a - a_0$ reads as

$$\dot{\tilde{a}} = \widetilde{G}\tilde{a} + \begin{bmatrix} \tilde{a}^T H^1 \tilde{a} \\ \vdots \\ \tilde{a}^T H^4 \tilde{a} \end{bmatrix} + \widetilde{B}\Gamma + \begin{bmatrix} (\overline{B}^1\Gamma)^T \tilde{a} \\ \vdots \\ (\overline{B}^4\Gamma)^T \tilde{a} \end{bmatrix}, \tag{4.1}$$

where a_0 is the equilibrium point computed for model (3.4) and

$$\widetilde{G} = G + \begin{bmatrix} a_0^T (H^1 + (H^1)^T) \\ \vdots \\ a_0^T (H^4 + (H^4)^T) \end{bmatrix}, \qquad \widetilde{B} = B + \begin{bmatrix} (\overline{B}^1)^T a_0 \\ \vdots \\ (\overline{B}^4)^T a_0 \end{bmatrix}. \tag{4.2}$$

Clearly, the modified model has the equilibrium at the origin, which is more convenient for controller design and stability analysis. The reader is referred to Caraballo et al. (2005) for a detailed description of the model simplification techniques.

Linear quadratic state feedback control

A linear approximation of (4.1) at the origin is readily obtained as

$$\dot{\tilde{a}} = \widetilde{G}\tilde{a} + \widetilde{B}\Gamma. \tag{4.3}$$

The eigenvalues of the unforced system have been computed as

$$\lambda(\widetilde{G}) = \begin{bmatrix} 1596.6 + 7023.1\text{i} \\ 1596.6 - 7023.1\text{i} \\ -3652 \\ -879.9 \end{bmatrix}. \tag{4.4}$$

The presence of two unstable conjugate eigenvalues implies, as expected, that the mean flow (corresponding to the equilibrium a_0) is an unstable solution for the Galerkin system (3.4).

Based on the linearized model (4.3), linear state feedback controller is a good candidate controller due to its advantage of pole assignment. This is also feasible in this research as it has been shown that the real

11

time estimate of the states of the Galerkin model (3.4) can be obtained via stochastic estimation method from real time pressure measurements (3.5). Linear-quadratic (LQ) optimal control offers a convenient and well-established methodology for the state feedback controller design. The linear system ($\widetilde{G}, \widetilde{B}$) has been tested to be controllable required for the LQ control design. LQ design calculates the optimal gain matrix K such that the state-feedback law

$$\Gamma(t) = -K\widetilde{a}(t),$$ (4.5)

minimizes the quadratic cost function

$$J_c(\widetilde{a}, \Gamma) = \int_0^\infty \left(\widetilde{a}^T W_{\widetilde{a}} \widetilde{a} + \Gamma^T W_\Gamma \Gamma\right) dt,$$ (4.6)

where $W_{\widetilde{a}} > 0$ and $W_\Gamma > 0$ are positive definite state and control weighting functions, respectively. Minimization of J_c results in moving $\widetilde{a}(t)$ to zero with as little control energy and state deviations as possible. In our design, the weights have been chosen as $W_{\widetilde{a}} = I_{4\times4}$ and $W_\Gamma = 1$, and the control gain reads as

$$K = \begin{bmatrix} -56.2176 & 8.8345 & -417.2384 & -12.7746 \end{bmatrix}.$$ (4.7)

Applying the state feedback control (4.5) to the linearized system (4.3) results in mirroring all the unstable right half plane eigenvalues of the linear system to the left half plane, as indicated in Fig. 6. Figure 7 shows the simulation results obtained by applying the state feedback control (4.5) to the finite-dimensional nonlinear model (3.4), which shows all the closed-loop states $a(t)$ have been quickly stabilized at the equilibrium point

$$a_0 = \begin{bmatrix} -0.5036 & 0.2788 & -0.1930 & 0.4980 \end{bmatrix}^T.$$ (4.8)

It can be concluded that, in principle, the LQ controller (4.5) designed from a linear approximated model (4.3) succeeds in stabilizing the equilibrium of the four-mode nonlinear Galerkin system (3.4).

Real time control results

Before presenting the experimental results, it is worth summarizing the structure of the model-based controller thus derived. As depicted in Fig. 8, the model-based controller includes a stochastic estimation subsystem and a feedback from the estimated state. In this study, quadratic stochastic estimation has been used to estimate the state $\hat{a}$ from the six real time pressure signals sensed at the locations shown in Fig. 2. It's interesting to notice that the estimate of the state $\hat{a}$ can be derived directly from pressure measurements by using equation (3.5). A saturation function and a constant scaling factor α play the same roles in the feedback loop as what have been presented in Caraballo et al. (2005). The largest possible scaling factor in this study has been found to be $\alpha = 0.265$, and the corresponding scaled control is in the form

$$\Gamma_\alpha(t) = -\alpha K \hat{a}(t).$$ (4.9)

The performance of the scaled control law (4.9) has been tested in closed-loop experiments for different flows in the neighborhood of Mach 0.3, the reference case for which the controller was designed. Figure 9 compares examples of SPL reduction obtained by the LQ state feedback control (left column) with open-loop optimal forcing control for the same flow conditions (right column) (Debiasi et. al. 2004) . The thin (red) line gives the SPL of the unforced (baseline) flow recorded at the center of the cavity (location 5 in Fig. 2), whereas the thick line corresponds to the SPL of the flow at the same location under state feedback control (blue) or optimal forcing control (green). The baseline flows at Mach 0.3 (a), Mach 0.27 (b), and Mach 0.32 (c) exhibit a strong, single-mode resonant peak. The frequency of this peak slightly increases with flow velocity from about 2700 to about 2900 Hz as

12

predicted by the Rossiter formula. For the designed case at Mach 0.3 (a), LQ control reduces the resonant peak by more than 15 dB, accompanied by the emergence of two additional peaks with frequencies around 2100 Hz and 3100 Hz, with lower SPL level than the original frequency. The same general characteristics and benefits are maintained when the control is applied to the lower Mach 0.27 flow (b) or to the higher Mach 0.32 one (c). Controlling the same flows with open-loop optimal forcing (right column) produces less noticeable reductions of the resonant peaks at Mach 0.30 and 0.27 and always introduces peaks at the forcing frequency higher than the highest spectral peaks with LQ control.

The scaled LQ state feedback control has been shown to successfully reduce the dominant Rossiter peak and have good robustness under different flow conditions, as shown by Fig. 9. The impact of the scaling factor α from the control systems point of view has been analyzed in our earlier paper (Caraballo et al. (2005). An improvement of the scaling factor from 0.05 to 0.265 has been achieved in this study. Relevant results are given in Figs. 10 and 11. As depicted in Fig. 10, we found the scaled LQ control with $\alpha = 0.265$ is still not a stabilizing controller although it has moved the closed-loop eigenvalues closer to the imaginary axis compare to the results given in Caraballo et al. (2005). Meanwhile, the scaled control with $\alpha = 0.265$ reduced the amplitude of the oscillations to a great extent as shown in Fig. 11. From the nonlinear point of view it can be observed in Fig. 11, though the scaled LQ control is not able to asymptotically stabilize the origin, it nevertheless provides a significant reduction of the amplitude of the limit cycle, as seen in Fig.11. The experimental results agree with this by showing a reduction of the amplitude of the Rossiter peak, Fig. 9.

The improvement we have achieved so far indicates that a richer model and a better estimation of the states are being used. In the future, we will continue to explore obtaining a richer model, which means to include more dynamics of the flow. On the other hand, a nonlinear dynamic observer will be pursued to improve estimation of the states of the Galerkin system.

V. CONCLUSIONS

The report presents the most recent progress made by the flow control group at the Collaborative Center of Control Science at The Ohio State University in the development of reduced-order model based feedback flow control. The DURIP grant made most of the effort possible. A large set of data composed of 1000 simultaneous PIV – pressure measurements were used to develop the feedback controller based on the reduced order model. The reduced-order model was obtained using the same methodology presented in our previous work, and is based on the use of snapshot based Proper Orthogonal Decomposition (POD) of PIV data in conjunction with Galerkin projection of the Navier-Stokes equations onto the POD eigenfunctions. The stochastic estimation method was used for real-time estimate of the time coefficients of the model from dynamic surface pressure measurements. It was observed that increasing the number of snapshots used for the derivation of the reduced order model improved the convergence of the model for the estimation of the time coefficients. The time coefficients for the model are oscillating around zero instead of about 1 as it did before. This suggests that the model is better predicting the experimental behavior of the flow. Equilibrium analysis led to the linearization of the reduced-order model around the equilibrium point. A simpler model for controller design was obtained by shifting the origin of the coordinates to the equilibrium point. This corresponds to removing the effect of the mean flow from the low-order model, and considering the local behavior of the system around the mean flow. The availability of real-time estimates of the state of the model allowed the use of linear state feedback control. To this aim we designed and tested experimentally a linear-quadratic optimal state feedback controller. From the results obtained we can conclude that the controller significantly reduces the resonance peak of the Mach 0.3 single-mode, for which it was designed, while introducing a couple of lower amplitude peak at 2100 Hz and 3100 Hz. As before, the controller seems to be quite robust, as it can control the flow with some variations in the flow Mach number. It was also noted that augmenting the number of snapshots used in the process increases the value of the scaling factor α for the real time implementation to values closer to unity suggesting that that the model is a better representation of the real flow. While, the current results are again quite encouraging and improved over our previous results, they could be further improved.

At the present, models based on snapshots from several forced flow cases and combination of flow cases are being developed and tested. The results obtained so far are promising, but further analysis, interpretation, and development are required. Additional methods for the control separation and multi-time estimation of the time coefficient are being pursued as well.

REFERENCES

1. Adrian, R. J., "On the Role of Conditional Averages in Turbulent Theory," Turbulence in Liquids, Science Press, Princeton, 1979.
2. Adrian, R. J., and Moin, P., "Stochastic estimation of organized turbulent structure: Homogeneous shear Flow," *Journal of Fluid Mechanics,* Vol. 190, 1988, pp. 531-559.
3. Caraballo, E., Samimy, M., and DeBonis, J., "Low Dimensional Modeling of Flow for Closed-Loop Flow Control," AIAA Paper 2003-0059, January 2003.
4. Caraballo, E., Malone, J., Samimy, M., and DeBonis, J., "A Study of Subsonic Cavity Flows - Low Dimensional Modeling," AIAA Paper 2004-2124, June 2004.
5. Caraballo, E., Yuan, X., Little, J., Debiasi, M., Yan, P. Serrani, A., Myatt, J., and Samimy, M., "Feedback Control of Cavity Flow Using Experimental Based Reduced Order Model," AIAA Paper 2005-5269, June 2005.
6. Caraballo, E., Yuan, X., Little, J., Debiasi, P. Serrani, A., Myatt, J., and Samimy, M., "Further Development of Feedback Control of Cavity Flow Using Experimental Based Reduced Order Model," AIAA Paper 2006-1405, January 2006.
7. Cattafesta III, L.N., Garg, S., Choudhari, M., and Li, F., "Active Control of Flow-Induced Cavity Resonance", AIAA Paper 97-1804, June 1997.
8. Cattafesta III, L. N., Williams, D. R., Rowley, C. W., and Alvi, F. S., "Review of Active Control of Flow-Induced Cavity Resonance," AIAA Paper 2003-3567, June 2003.
9. Cole, D. R., Glauser, M. N., and Guezennec, Y. G., "An Application of the Stochastic Estimation to the Jet Mixing Layer," *Physics of Fluids*, Vol. 4, No. 1, 1991, pp. 192-194.
10. Debiasi, M. and Samimy, M., "Logic-Based Active Control of Subsonic Cavity Flow Resonance," *AIAA Journal*, Vol. 42, No. 9, pp. 1901-1909, September 2004.
11. Debiasi, M., Little, J., Malone, J., Samimy, M., Yan, P., and Özbay, H., "An Experimental Study of Subsonic Cavity Flow – Physical Understanding and Control," AIAA Paper 2004-2123, June 2004.
12. Delville, J., Cordier, L. and Bonnet, J.P., "Large-Scale-Structure Identification and Control in Turbulent Shear Flows," In Flow Control: Fundamentals and Practice, edited by Gad-el-Hak, M., Pollard A. and Bonnet, J., Springer-Verlag, 1998, pp. 199-273.
13. Gad-el-Hak, M., Flow Control – Passive, Active, and Reactive Flow Management, Cambridge University Press, New York, NY, 2000.
14. Glauser, M. N., Higuchi, H., Ausseur, J., and Pinier, J., "Feedback Control of Separated Flows (Invited)," AIAA Paper 2004-2521, June 2004.
15. Heller, H. H., and Bliss, D. B., "The Physical Mechanisms of Flow-Induced Pressure Fluctuations in Cavities and Concepts for their Suppression," AIAA Paper 75-491, March 1975.
16. Holmes, P., Lumley, J.L., and Berkooz, G., "Turbulence, Coherent Structures, Dynamical System, and Symmetry," Cambridge University Press, Cambridge, 1996.
17. Lumley, J. "The Structure of Inhomogeneous Turbulent Flows", Atmospheric Turbulence and wave propagation. Nauca, Moscow. 1967 166-176.
18. Noack, B., Tadmor, G., and Morzynski, M. ., "Low-Dimensional Models for Feedback Flow Control. Part I: Empirical Galerkin Models," AIAA Paper 2004-2408, June 2004.
19. Picard, C., and Delville, J., "Pressure Velocity Coupling in a Subsonic Round Jet," *International Journal of Heat and Fluid Flow*, Vol. 21, pp. 359-364, 2000.
20. Rossiter, J.E., "Wind Tunnel Experiments on the Flow Over Rectangular Cavities at Subsonic and Transonic Speeds", RAE Tech. Rep. 64037, 1964 and Aeronautical Research Council Reports and Memoranda No. 3438, Oct. 1964.

21. Rowley, C. W., "Modeling, Simulation and Control of Cavity flow Oscillations", Ph.D. thesis, California Institute of Technology. 2002.

22. Samimy, M., Debiasi, M., Caraballo, E., Malone, J., Little, J., Özbay, H., Efe, M. Ö., Yan, P., Yuan, X., DeBonis, J., Myatt, J. H., and Camphouse, R. C., "Exploring Strategies for Closed-Loop Cavity Flow Control," AIAA Paper 2004-0576, January 2004.

23. Siegel, S., Cohen, K., Seidel, J., and McLaughlin, T., "Tow Dimensional Simulations of a Feedback Controlled D-Cylinder Wake," AIAA Paper 2005-5019, June 2005.

24. Sirovich, L. "Turbulence and the Dynamics of Coherent Structures", *Quarterly of Applied Math.* Vol. XLV, N. 3, 1987, pp. 561-590.

25. Thurow, B. S., Jiang, N., Lempert, W. R., and Samimy, M., "Development of Megahertz-Rate Planar Doppler Velocimetry for High-Speed Flows," *AIAA Journal*, Vol. 43 N° 3, March 2005, pp. 500-511.

26. Ukeiley, L., and Murray, N., "Velocity and Surface Pressure Measurements in an Open Cavity," *Exp. In Fluids*, Vol. 38, 2005, pp. 656-671.

27. Yuan, X. , Caraballo, E., Yan, P., Özbay, H., Serrani, A., DeBonis, J., Myatt, J. H. and Samimy, M., "Reduced-Order Model-Based Feedback Controller Design for Subsonic Cavity Flows", AIAA Paper 2005-0293, January 2005.

FIGURES
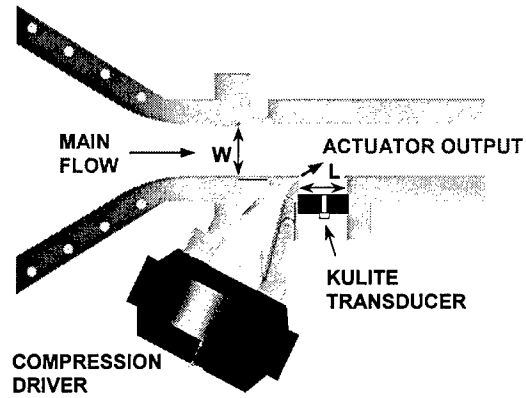
Fig. 1: Scaled drawing of the experimental set up showing the incoming flow, the actuation location (at the receptivity location of the free shear layer formed over the cavity), and other geometrical details.
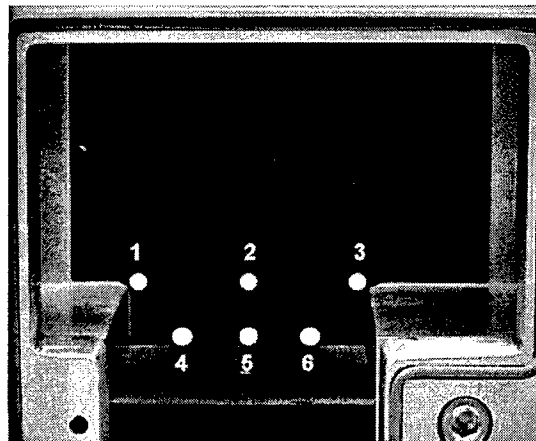

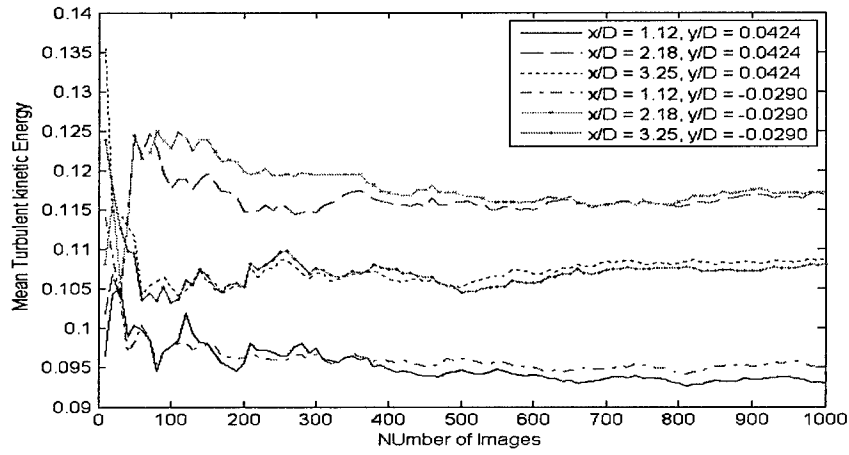Fig. 2: Location of Kulite pressure transducers in the cavity flow.

Fig. 3: Mean turbulent kinetic energy of the cavity flow at different locations of the shear layer.
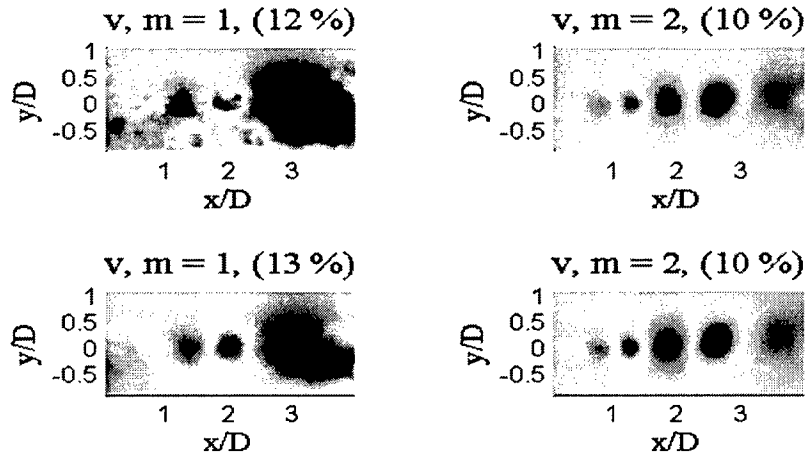

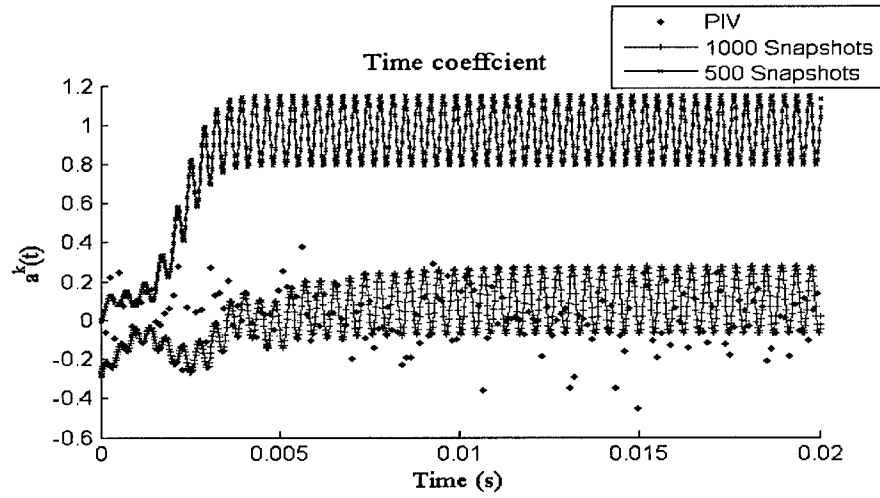Fig. 4: First two POD modes for the cavity flow. Top 500 Snapshots. Bottom 1000 snapshots.

18

Fig. 5: First time coefficient form GS. Black (dots) PIV, Red (+) 1000 Snapshots and Blue (x) 500 Snapshots.
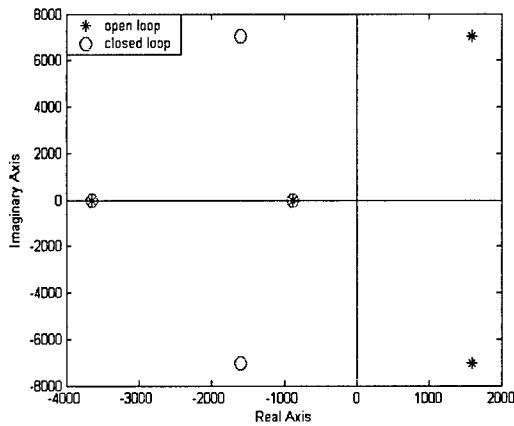
Fig. 6: Eigenvalues of the open loop system and closed loop system.
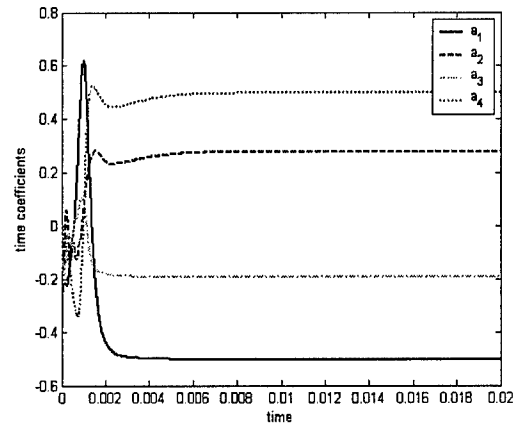
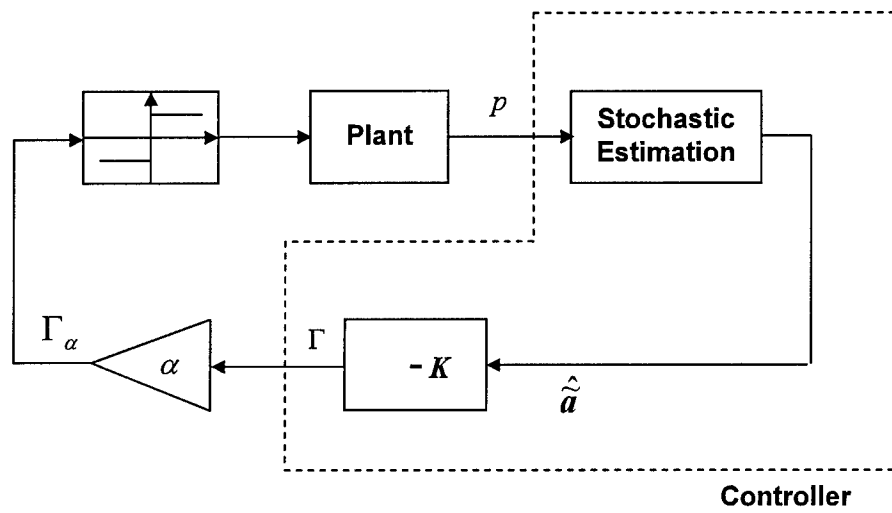**Fig. 7: Time coefficient solutions of the closed loop simulation results.**

19

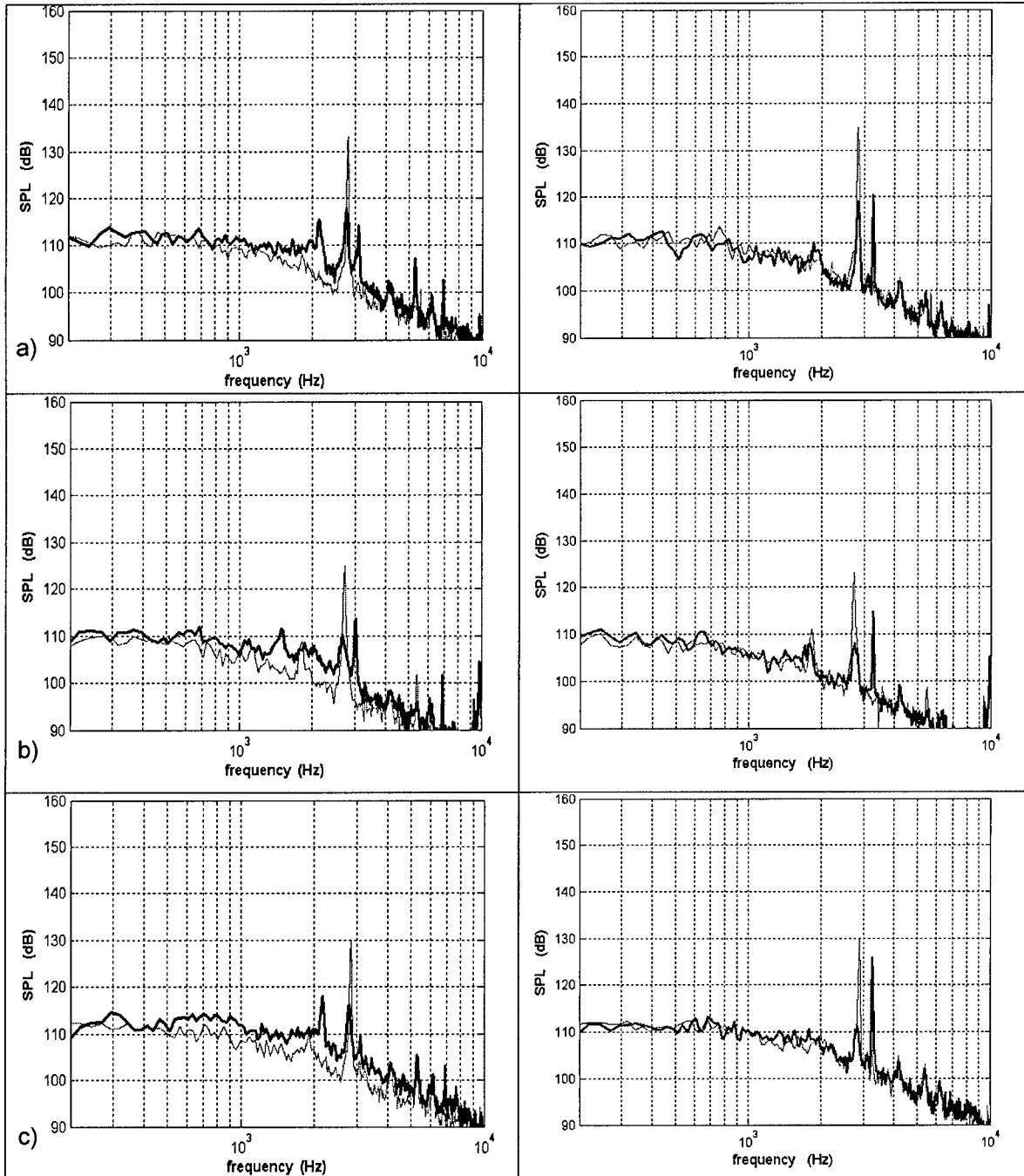**Fig. 8: Diagram of the closed loop system with LQ state feedback control.**

Figure 9: Effect of LQ control with 4 modes (left plots) and of optimal open loop forcing (right) on cavity flow with different Mach number; thin (red) line is the unforced flow SPL spectrum and thick (blue or green) line is the spectrum with control at: a) Mach 0.30 (design condition); b) Mach 0.27; c) Mach 0.32.
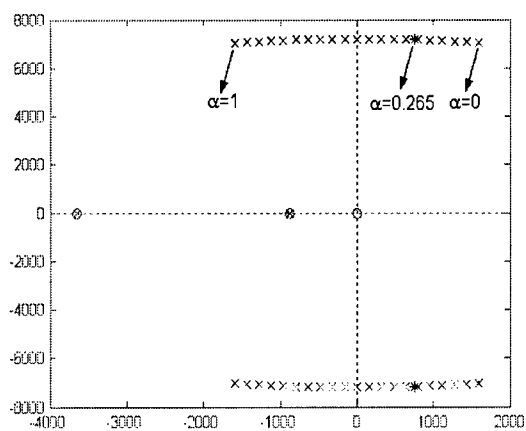
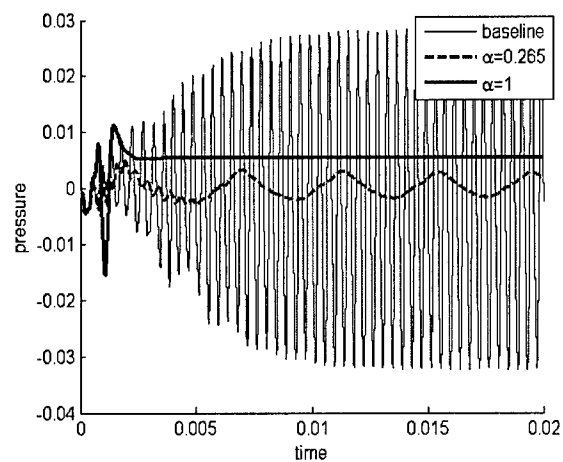**Fig. 10. Eigenvalues of the closed loop systems with different scaling factor α.**

Fig. 11: Closed loop responses at P_3 with different scaling factor α.